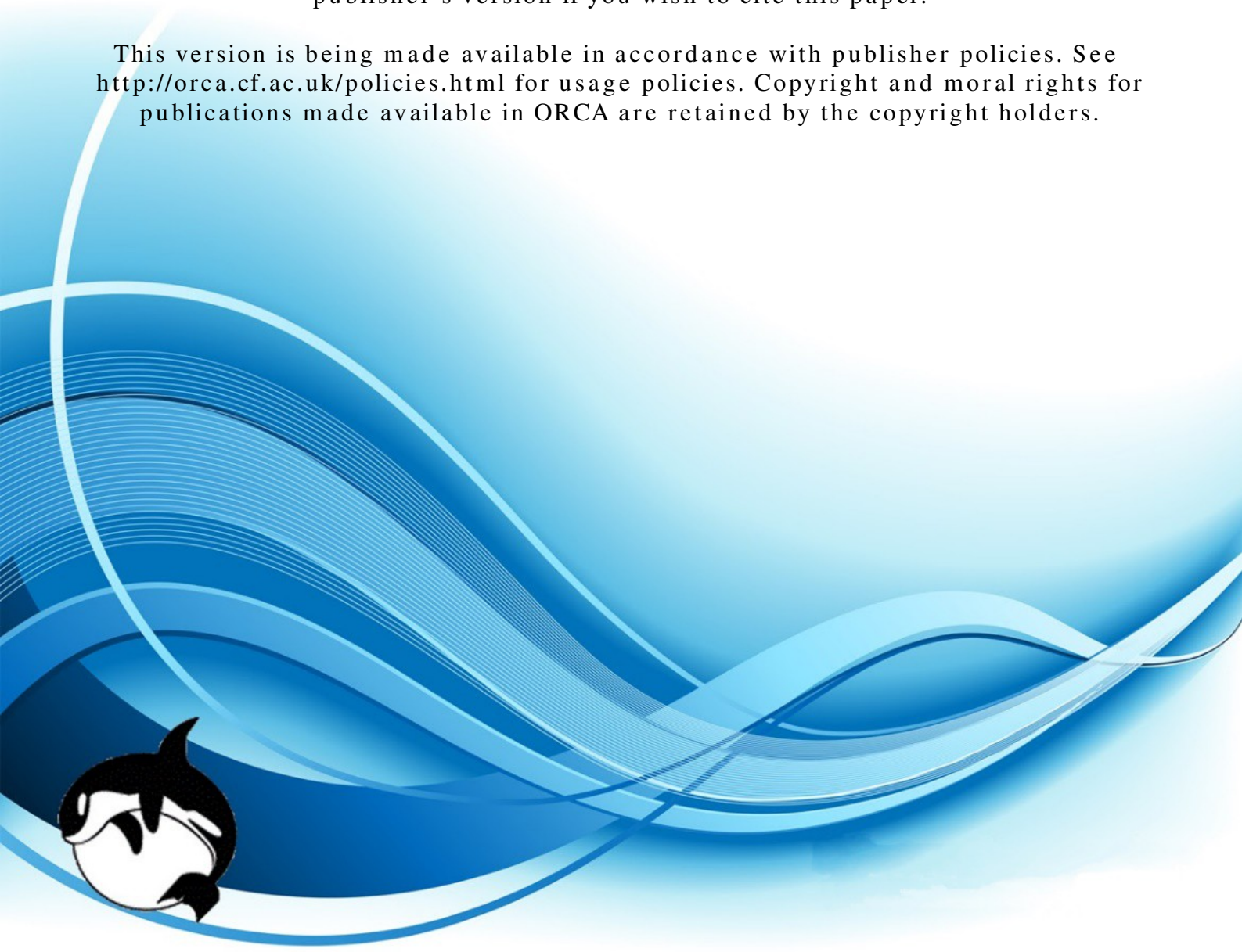

Global dryland self-expansion enabled by land–atmosphere feedbacks

Akash Koppa[1*], Jessica Keune[1,2], Dominik L. Schumacher[3], Katerina Michaelides[4,5], Michael Singer[5,6], Sonia I. Seneviratne[3], Diego G. Miralles[1]

Affiliations:

[1]Hydro-Climate Extremes Lab (H-CEL), Ghent University, Ghent, Belgium.

[2]European Centre for Medium-Range Weather Forecasts, Bonn, Germany.

[3]Department of Environmental Systems Science, Institute for Atmospheric and Climate Science, ETH Zurich, Zurich, Switzerland.

[4]School of Geographical Sciences, University of Bristol, Bristol, United Kingdom.

[5]Earth Research Institute, University of California Santa Barbara, Santa Barbara, United States of America.

[6]School of Earth and Environmental Sciences, Cardiff University, Cardiff, United Kingdom.

*Corresponding author. Email: akash.koppa@ugent.be

Abstract: Dryland expansion threatens widespread water scarcity and biodiversity loss. While the drying influence of global warming is well established, the role of existing drylands in their own expansion is relatively unknown. Here, by tracking the air flowing over drylands, we show that the warming and drying of that air contributes to dryland expansion in the downwind direction. As they dry, drylands contribute less moisture and more heat to downwind humid regions, reducing precipitation and increasing atmospheric water demand, which ultimately causes their aridification. Globally, 43.7±33% of the observed increase in aridity over regions that underwent a humid–dry transition in 1981–2018 occurred due to self-expansion. Our results corroborate the urgent need for climate change mitigation measures in drylands to decelerate their expansion.

One-Sentence Summary: Drylands are fueling their own expansion by drying and warming the air in their surroundings.

Main Text: Drylands are typically defined as regions in which the atmospheric water demand (potential evaporation, E_p) significantly exceeds supply (precipitation, P). Currently, they occupy ~45% of the Earth's land surface (*1*), and are widely recognized as hotspots of climate change (*2*), yet it remains unclear how the global distribution of drylands will evolve under a changing climate. From an atmospheric aridity perspective (often represented by the Aridity Index, hereby $AI = E_p/P$), there is strong evidence of intensified aridification of existing drylands and their expansion into more humid regions (*3–6*). Debates persist around whether an atmosphere-centric metric of aridity, such as AI, is appropriate for identifying drylands and quantifying their expansion, especially under rising atmospheric CO_2, given the potentially beneficial influence of CO_2 fertilization on vegetation primary productivity and water use efficiency (*7–10*), and the fact that actual evaporation may not increase with E_p due to soil moisture limitation (*11*, *12*). However, the degree to which increasing CO_2 concentrations can counteract the effects of atmospheric aridity on vegetation remains uncertain (*13–16*), particularly in drought conditions (*17*, *18*). Moreover, field experiments, observations, and model-based studies have established unequivocal links between atmospheric aridity and adverse changes in water availability (*19–21*), ecosystem function (*22*), stability of soils (*6*), and nutrient cycling (*23*). Therefore, it is vital to improve our understanding of the processes that drive increases in atmospheric aridity over humid regions, and which ultimately result in dryland expansion.

From an atmospheric perspective, dryland expansion is assumed to take place when AI surpasses a threshold of 1.55, representing a shift form the humid to the dry subhumid class, as defined by the World Atlas of Desertification (*24*). This occurs when P becomes lower than 65% of E_p, or E_p becomes larger than P by more than 55% for a prolonged period (a minimum of 10 years in this study). Changes in E_p are inextricably linked to increasing temperature under rising greenhouse gases and associated changes in relative humidity and vapor pressure deficit (*25–29*). E_p has experienced significant positive trends in historical records (*30–32*) and is projected to further increase in the future (*33*, *34*), thus driving ecosystems into a more arid regime worldwide (*35–41*). While E_p increases are largely consistent with temperature trends, changes in P and their potential drivers are more complex. In the long-term, global warming can alter the atmospheric water holding capacity, its stability, and large-scale circulation patterns (*42–44*), resulting in systematic changes in the spatiotemporal patterns of P. Because of these complex changes, simple paradigms such as 'dry gets drier and wet gets wetter' are unable to accurately explain the observed trends in P over land, especially in transitional regimes on the edge between drylands and humid regions (*12*, *45*).

At subseasonal to seasonal time scales, the causes of P deficits are better understood; anomalous anticyclonic conditions created by shifts in global circulation patterns, often associated with anomalies in sea surface temperatures, can cause deficits in P, which can then potentially evolve into a drought (*46–48*). Then, the land dry-out can reinforce P deficits and E_p increases, through what is typically referred to as positive land–atmosphere feedbacks (*49–52*): deficits in P lead to drier soil and vegetation, often resulting in a decreased moistening (through evaporation, E) and increased warming (through sensible heat flux, H) of the air, which, in turn, reduces precipitable water and increases E_p (*49*). Moreover, these land feedbacks can influence the atmosphere of downwind regions through advection of a) drier air leading to a reduction in the total moisture available for P (*53*) and b) warmer air leading to an increase in air temperature and consequently E_p (*54*, *55*). However, the degree to which the downwind propagation of P deficits and E_p increases caused by land–atmosphere feedbacks in upwind drylands can contribute to the aridification of humid environments (i.e., expansion of drylands) over the multi-annual timescales at which aridification occurs, remains unknown.

Herein, we investigate the role of drylands in the aridification of downwind humid regions over multiple decades and across the global land surface. We hypothesize that drylands contribute to their own expansion through land–atmosphere feedbacks, leading to the aridification of downwind humid regions, a process we term here as 'dryland self-expansion'. We quantify the importance of this process by spatiotemporally tracking the atmospheric moisture and heat transported into humid–dry transitioning regions using 38 years (1981–2018) of simulations from an observationally-constrained Lagrangian atmospheric transport model (methods in (*56*)). While reductions in moisture transported through drier air can affect P (eq. S5), increased heat transport through warmer air can affect E_p (eqs. S6 and S7) via changes in air temperature and vapor pressure deficit. Therefore, using the Lagrangian model, we can trace the origins of both the observed P deficits and E_p increases that drive the aridification of downwind humid regions and isolate the importance of upwind drylands. In addition, we quantify the changes in the land surface fluxes within upwind drylands that initiate and promote their self-expansion.

Global dryland expansion. Between 1981 and 2018, ~5.2 million km^2 of humid land transitioned into a dryland (table S1). Accounting for dryland contraction (~1.3 million km^2), this represents a ~9% expansion in global dryland area. Long-term expansion into humid regions is observed in all major drylands across the globe, with Eurasia witnessing the largest, followed by Africa and South America (Fig. 1 and table S1). In relative terms, the area of the Caatinga has expanded by a remarkable 78.9%, followed by the South American drylands (25.7%) (table S1). These patterns are consistent with recent studies which have documented drying trends in the southwest of the United States of America (*57*), Congo (*58*), Central Asia (*59*), and Caatinga (*60*). On the other hand, the largest dryland contraction of ~0.5 million km^2 is observed in North America and eastern Eurasia (fig. S1 and table S1). Dryland expansion and contraction is concentrated in regions bordering existing drylands, as expected. Likewise, we see a large variance in the degree of aridification, with AI increasing by up to 60% in parts of the Caatinga (fig. S2).

Decomposing the increase in aridity into its first order drivers (P and E_p) (refer to (*56*) for methods), we find that, globally, the relative contribution of changes in P (54.9$\pm$26%) is larger than that of E_p (45.1$\pm$26%). However, the relative importance of P and E_p expresses high spatial variability across the globe (Fig. 2); while decreases in P play a more important role in South America (*61*) and Africa (*62*), increases in E_p explain most of the aridification in the western parts of Eurasia (figs. S3 and S4). These spatial patterns are primarily driven by P changes, which show much higher variance than those in E_p. Nevertheless, several regions underwent a humid–dry transition despite experiencing small increases in P, which were thus counteracted by disproportionate increases in E_p (Q1 and Q2 in Fig. 2) (*63*).

Contribution of dryland self-expansion. Using a Lagrangian atmospheric model constrained by reanalysis and observation-based estimates of P and E (*64*) (refer to (*56*)), we quantify the contribution of existing drylands to their own expansion. Globally, 43.7$\pm$33% of the increase in aridity over humid regions transitioning into dryland is caused by the self-expansion of existing drylands (Fig. 1). In parts of Australia and Eurasia, self-expansion is the dominant mechanism by which drylands spread (fig. S8), accounting for >50% of the aridity increase. We also see strong intra-regional variability in the importance of self-expansion, especially in Africa, Caatinga, and the eastern parts of Eurasia (fig. S8). While the drying of the Congo bordering the East Sudanian savanna is primarily driven by self-expansion, this mechanism plays a less significant role in the expansion of the East African drylands. Similarly, we observe an increasing importance of self-expansion from north to south in the Caatinga and from east to west in eastern Eurasia (fig. S8).

Furthermore, we find that more than half of the global self-expansion is due to the reduction in P contribution from upwind drylands (Fig. 1). However, this relative importance of P for self-expansion is highly variable across different regions, accounting for only 30% of the self-expansion in western Eurasia but up to 82% in Australia (fig. S9). While self-expansion in the sub-tropics and the Southern Hemisphere drylands is primarily driven by reductions in upwind P contributions (fig. S9), increases in E_p are the major cause of self-expansion in the mid-latitude drylands of the Northern Hemisphere (fig. S10), consistent with the importance of P and E_p changes to increase in aridity in these regions.

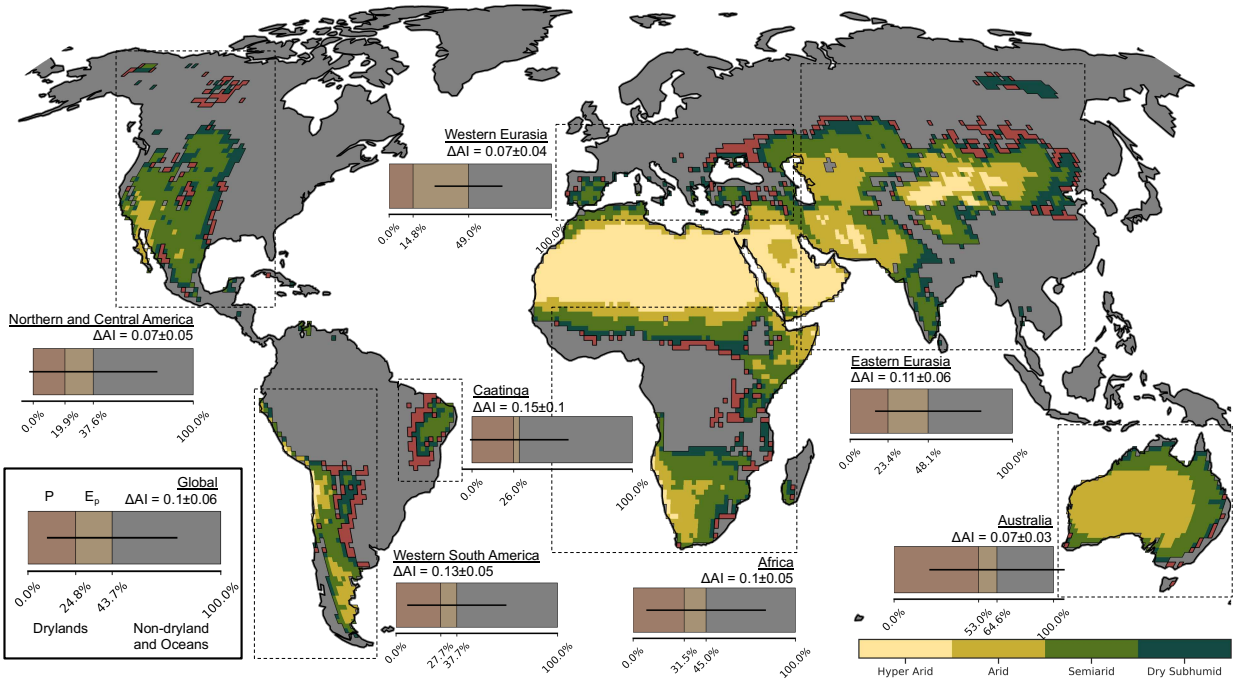

Fig. 1. Global prevalence of dryland self-expansion. Global map of existing (shades of green) and expanding (red) drylands. The stacked barplots show the degree to which the increase in aridity index (*Δ*AI) over the expanded drylands can be attributed to reduced P (brown) and increased E_p (tan) from existing drylands (self-expansion) and other regions (grey), across the globe. The uncertainty bar represents one standard deviation in the combined importance of the changes in P and E_p contributions from upwind drylands to their self-expansion. The extent of the upwind drylands corresponds to the year 1980. The expanding dryland regions are estimated over the period 1981–2018. The aridity thresholds used for the classification of drylands are presented in *(56)*.

Moisture and heat transport as a conduit of dryland self-expansion. In regions with a high climatological dependency on oceans and upwind humid lands for their supply of moisture (affecting P), and heat (affecting E_p), there is relatively low influence of dryland self-expansion. For example, the lower influence of self-expansion in regions such as East Africa can be attributed to the predominance of the ocean as a major source of moisture and heat (*65*). Similarly, in regions where self-expansion plays a relatively small role such as the Caatinga, South America, and West Eurasia, a large proportion of the imported moisture and heat can be traced to the ocean and humid land areas (tables S2 and S3). In such regions, drylands have expanded into ~0.9 million km^2 of humid land, despite an increase in P contribution or a decline in E_p contribution from upwind drylands, i.e., without self-expansion (Q3 in Fig. 2, fig. S25, and fig. S26). However, in some regions upwind drylands play a disproportional role in downwind aridification despite their importance as a source of moisture and heat to these regions being low. For example, in Australia, 64.6% of the total increase in aridity is caused by self-expansion (Fig. 1) but climatologically, upwind drylands contribute only ~19% to total P and ~41% to total E_p on

average (table S2 and table S3). Furthermore, in eastern Eurasia, for example, upwind drylands play an important role in dryland expansion (Fig. 1), even though humid regions form the primary source of both heat and moisture (Table S2 and S3). In most regions transitioning from humid to dryland, we found both declines in P and increases in E_p contributions from existing upwind drylands (Fig. 2 and figs. S18–S24). This raises the question: What causes the reduction in moisture and the increase in heat transport from upwind drylands into downwind humid regions, resulting in their P deficits and E_p surpluses, and thus dryland self-expansion?

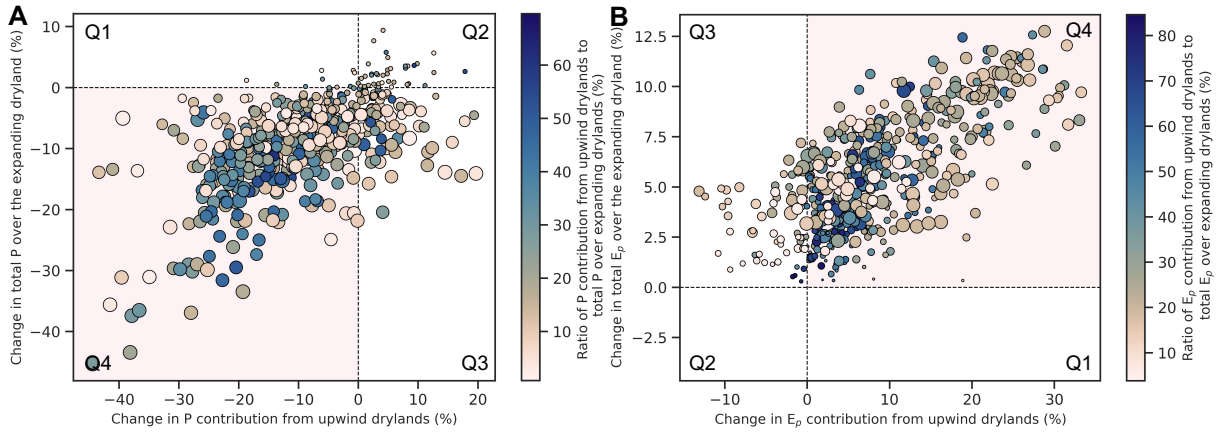

Fig. 2. Relative importance of changes in P and E_p contribution from upwind drylands in their expansion. Relationship between percentage change in total P (**A**) or E_p (**B**) over expanding drylands (y-axis) and the change in P (**A**) or E_p (**B**) contribution from upwind drylands to the expanding drylands (x-axis). Each marker represents a 1°x1° grid cell which has undergone a humid–dry transition, and over which the Lagrangian model simulations are evaluated to estimate P and E_p contributions from upwind drylands. In total, the 540 grid cells represent ~5.2 million km^2 of transitioning land. The color of each marker represents the mean contribution of upwind drylands to the total P and E_p in grid cells undergoing a humid–dry transition, calculated over the entire period of study (1981–2018). The size of the marker represents the importance of changes in P and E_p to the increase in aridity over the drying humid regions; big markers indicating high importance and small markers indicating low importance. Regions in quadrants Q1 and Q2 have undergone a humid-dry transition despite local net increases in P (**A**) or decreases in E_p (**B**). Regions in quadrant Q1 have undergone a net increase in P (**A**) or decrease in E_p (**B**) despite a reduction in P (**A**) or an increase in E_p (**B**) contribution from upwind drylands. Regions in quadrants Q3 and Q4 have undergone a humid-dry transition due to a local reduction in P (**A**) or an increase in E_p (**B**). Regions in Q3 have witnessed a reduction in P (**A**) or an increase in E_p (**B**), despite an increase in P (**A**) or a decrease in E_p (**B**) contribution from upwind drylands i.e., no dryland self-expansion. Regions in Q4 have experienced a reduction in P (**A**) or a decrease in E_p (**B**) partially due to a reduction in P (**A**) or increase in E_p (**B**) contribution from upwind drylands i.e., dryland self-expansion.

Upwind dryland aridification as a driving force of self-expansion. Here, we hypothesize that changes in P and E_p over expanding drylands result mainly from the aridification of upwind drylands, causing long-term changes in their land–atmosphere fluxes i.e., reduction in E and increase in H. To test the hypothesis, we group the upwind drylands into two clusters – drying and wetting – based on whether they have become more arid or humid during the period in which the downwind humid areas transitioned into drylands. Then, we compare the changes in upwind P and E_p contributions of both clusters (i.e., upwind drying and wetting drylands) to the AI of expanding drylands. Despite comparable areas of existing drylands undergoing drying (~29 million km^2) and wetting (~27 million km^2) (fig. S29), we find that the changes in P and E_p contributions to downwind aridification are an order of magnitude larger when upwind drylands experienced a drying trend (Fig. 3c and 3d), corroborating the importance of (upwind) dryland aridification for dryland self-expansion. While P contributions to AI from drying upwind drylands are largely negative (mean of -16.1 ± 21.5 mm year^{-1}), the P contributions to AI changes

from wetting drylands do not show significant changes (mean of –0.3±6.0 mm year^{-1}). For example, the P contribution of the wetting western part of Australia (fig. S29) experienced an increase, while that of the drying eastern part experienced a decline (fig. S19). A similar conclusion can be drawn for the P contribution to dryland self-expansion from East Africa and southwestern United States, which have both witnessed unprecedented warming and aridification (*66*, *67*). Likewise, the change in E_p contributions to AI from drying drylands is clearly positive (18.0±18.7 mm year^{-1}). However, changes in E_p contributions from wetting drylands show a larger spread and less positive values (mean of 3.7±8.5 mm year^{-1}). This is particularly evident in the increased sensible heat contribution from the Sahara, which has witnessed both drying and wetting (fig. S29), to dryland expansion in not only Africa but also eastern and western parts of Eurasia (figs. S18, S21, and S22).

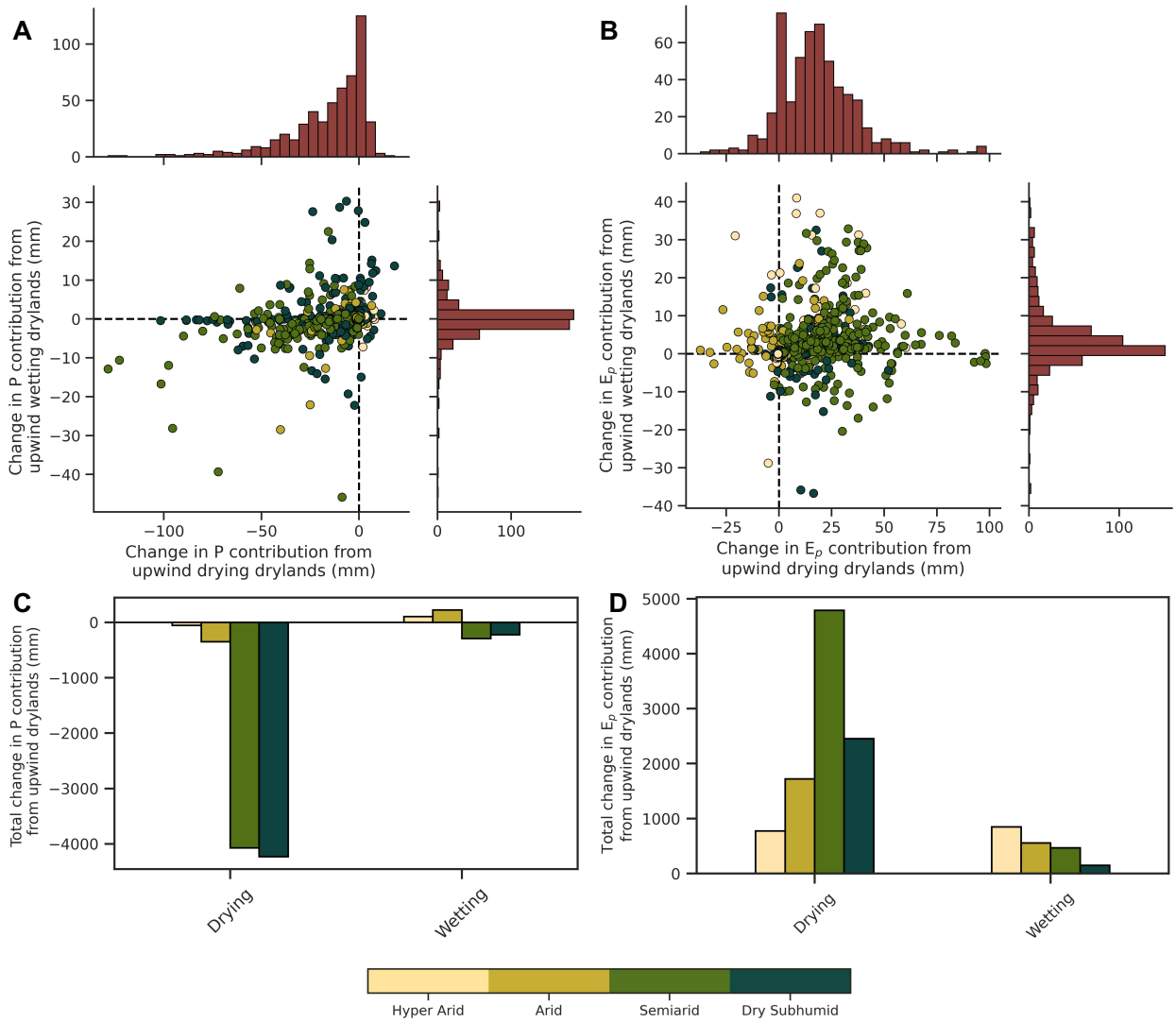

Fig. 3. Relative importance of drying and wetting upwind drylands for self-expansion. Comparison of change in P (**A**) and E_p (**B**) contributions from upwind drylands, which are either drying (x-axis) or wetting (y-axis), to downwind regions which are undergoing a humid–dry transition. The color of each point refers to the aridity class (hyper arid, arid, semiarid, or dry subhumid) from which the maximum change in P or E_p contribution arises. The bar plots show the total change in P (**C**) and E_p (**D**) contribution from drying and wetting upwind drylands (classified according to aridity classes detailed in *(56)*) to all the downwind regions undergoing a humid–dry transition i.e, changes in P and E_p contributions from upwind drylands with different aridity classes have been summed up for all the 540 grid cells amounting to ~5.2 million km^2 of land area.

Furthermore, we see that a major proportion of the changes in P and E_p contributions globally can be attributed to semiarid and dry subhumid regions that have experienced a drying trend (Fig. 3). The large difference between the contributions of upwind drying and wetting drylands to self-expansion is due to the contrasting changes in land–atmosphere fluxes within them (fig. S30). We find that changes in both E (figs. S30a–e) and H (fig. S30f) fluxes are significantly different between drying and wetting drylands, during the period in which downwind humid regions transitioned into a dryland. While H has witnessed a nominal decline in wetting drylands (–0.5±10.8%), it is substantially increased in their drying counterparts (5.9±9.1%). Changes in E follow a similar pattern, with reductions in drying drylands (–3.4±12.1%) and substantial increases in wetting drylands (12.3±26.7%). Importantly, we see that land E is increasingly unable to satisfy the increased atmospheric demand for water, with the ratio of E to E_p reducing by –6.1±5.7% in drying drylands compared to a minor increase of 0.3±6.9% in wetting drylands (fig. S30). We note that the increased atmospheric water demand in upwind drylands is also a consequence of higher H. Therefore, changes in land–atmosphere fluxes, and subsequent advection, provide a mechanistic pathway for the downwind propagation of aridification.

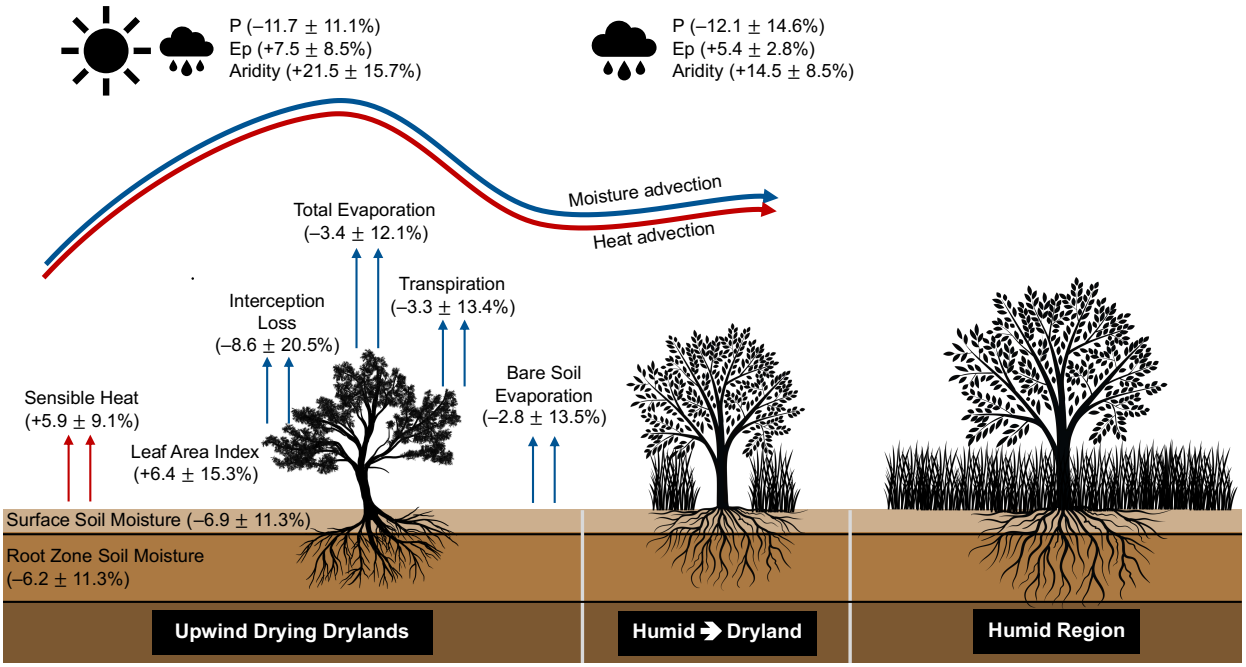

Figure 4. Conceptual representation of the dryland expansion process. Aridification of upwind drylands due to both declines in P and increases in E_p leads to negative changes in soil water availability, which in turn results in changes in land–atmosphere fluxes. The reduced evaporation and increased sensible heat fluxes dry and warm the air in upwind drylands which when advected downwind results in P declines and E_p surpluses over downwind humid regions, and ultimately contributing to dryland expansion. The numbers represent the global mean changes in various hydroclimatic variables in upwind drylands which are drying and the regions undergoing a humid–dry transition, estimated over the period 1981–2018. The average and uncertainty estimate (standard deviation) of surface fluxes (sensible heat, total evaporation, interception loss, transpiration, and bare soil evaporation), leaf area index (LAI), and soil moisture (surface and root zone) over upwind drylands are weighted by their contribution to the precipitation and potential evaporation over downwind regions undergoing a humid–dry transition.

Synthesis of the dryland self-expansion process and implications. Progressive aridification of existing drylands, initiated by global warming (*2*, *68*), is the primary trigger for dryland self-expansion (Fig. 4). Specifically, long-term declines in P and increase in E_p over drylands

desiccate vegetation and soils, which in turn reduces evaporation (*69*). We see decreases in all components of evaporation, including transpiration, interception loss, and bare soil evaporation (Fig. 4). These declines occur despite the greening of drylands seen in our results (LAI increase of 6.4±15.3% in drying and 18.8±25.1% in wetting drylands, respectively) (fig. S31) and in previous assessments (*70*, *71*). Deficits in E are accompanied by an increase in H. These changes in both E and H are then propagated through the advection of a drier and warmer air, respectively, to downwind humid regions, resulting in deficits in P and surpluses in E_p. The persistence of this process over a sufficiently long period of time leads to expansion of drylands in the downwind direction. Thus, our results uncover a land–atmosphere feedback process by which drylands may have spatially evolved historically and provide a theoretical framework for predicting their future expansion. With the projected increase in atmospheric aridity (*51*) and soil moisture desiccation (*72*), coupled with potential saturation of vegetation greening (*15*), the dryland self-expansion mechanism elucidated here is expected to increase in relevance in the future. Here, not only do we identify regions which are vulnerable to gradual and abrupt regime shifts, but we also identify the upwind regions that are responsible for the aridification. Thus, our results provide a scientific basis to help identify and design regionally targeted ecosystem management strategies in existing drylands to slow down their rates of drying and consequent expansion.

References and Notes

1. D. S. Schimel, Drylands in the Earth System. *Science (1979)* **327**, 418–419 (2010).
2. L. Wang, W. Jiao, N. MacBean, M. C. Rulli, S. Manzoni, G. Vico, P. D'Odorico, Dryland productivity under a changing climate. [Preprint] (2022). https://doi.org/10.1038/s41558-022-01499-y.
3. S. Feng, Q. Fu, Expansion of global drylands under a warming climate. *Atmos. Chem. Phys* **13** (2013).
4. C. Zhang, Y. Yang, D. Yang, X. Wu, Multidimensional assessment of global dryland changes under future warming in climate projections. *J Hydrol (Amst)* **592** (2021).
5. A. G. Koutroulis, Dryland changes under different levels of global warming. *Science of the Total Environment* **655** (2019).
6. J. Huang, H. Yu, X. Guan, G. Wang, R. Guo, Accelerated dryland expansion under climate change. *Nat Clim Chang* **6** (2016).
7. A. Berg, K. A. McColl, No projected global drylands expansion under greenhouse warming. *Nat Clim Chang* **11** (2021).
8. X. Lian, S. Piao, A. Chen, C. Huntingford, B. Fu, L. Z. X. Li, J. Huang, J. Sheffield, A. M. Berg, T. F. Keenan, T. R. McVicar, Y. Wada, X. Wang, T. Wang, Y. Yang, M. L. Roderick, Multifaceted characteristics of dryland aridity changes in a warming world. [Preprint] (2021). https://doi.org/10.1038/s43017-021-00144-0.
9. P. C. D. Milly, K. A. Dunne, Potential evapotranspiration and continental drying. *Nature Climate Change 2016 6:10* **6**, 946–949 (2016).
10. M. L. Roderick, P. Greve, G. D. Farquhar, On the assessment of aridity with changes in atmospheric CO2. *Water Resour Res* **51**, 5450–5463 (2015).
11. S. I. Seneviratne, T. Corti, E. L. Davin, M. Hirschi, E. B. Jaeger, I. Lehner, B. Orlowsky, A. J. Teuling, Investigating soil moisture-climate interactions in a changing climate: A review. [Preprint] (2010). https://doi.org/10.1016/j.earscirev.2010.02.004.
12. P. Greve, B. Orlowsky, B. Mueller, J. Sheffield, M. Reichstein, S. I. Seneviratne, Global assessment of trends in wetting and drying over land. *Nature Geoscience 2014 7:10* **7**, 716–721 (2014).
13. A. J. Winkler, R. B. Myneni, A. Hannart, S. Sitch, V. Haverd, D. Lombardozzi, V. K. Arora, J. Pongratz, J. E. M. S. Nabel, D. S. Goll, E. Kato, H. Tian, A. Arneth, P. Friedlingstein, A. K. Jain, S. Zaehle, V. Brovkin, Slowdown of the greening trend in natural vegetation with further rise in atmospheric CO2. *Biogeosciences* **18**, 4985–5010 (2021).
14. W. Peters, I. R. van der Velde, E. van Schaik, J. B. Miller, P. Ciais, H. F. Duarte, I. T. van der Laan-Luijkx, M. K. van der Molen, M. Scholze, K. Schaefer, P. L. Vidale, A. Verhoef, D. Wårlind, D. Zhu, P. P. Tans, B. Vaughn, J. W. C. White, Increased water-use efficiency and reduced CO2 uptake by plants during droughts at a continental scale. *Nature Geoscience 2018 11:10* **11**, 744–748 (2018).

15. S. Wang, Y. Zhang, W. Ju, J. M. Chen, P. Ciais, A. Cescatti, J. Sardans, I. A. Janssens, M. Wu, J. A. Berry, E. Campbell, M. Fernández-Martínez, R. Alkama, S. Sitch, P. Friedlingstein, W. K. Smith, W. Yuan, W. He, D. Lombardozzi, M. Kautz, D. Zhu, S. Lienert, E. Kato, B. Poulter, T. G. M. Sanders, I. Krüger, R. Wang, N. Zeng, H. Tian, N. Vuichard, A. K. Jain, A. Wiltshire, V. Haverd, D. S. Goll, J. Peñuelas, Recent global decline of CO2 fertilization effects on vegetation photosynthesis. *Science (1979)* **370**, 1295–1300 (2020).
16. F. Li, J. Xiao, J. Chen, A. Ballantyne, K. Jin, B. Li, M. Abraha, R. John, Global water use efficiency saturation due to increased vapor pressure deficit. *Science* **381**, 672–677 (2023).
17. I. P. on C. C. (IPCC), Global Carbon and Other Biogeochemical Cycles and Feedbacks. *Climate Change 2021 – The Physical Science Basis*, 673–816 (2023).
18. I. P. on C. C. (IPCC), Weather and Climate Extreme Events in a Changing Climate. *Climate Change 2021 – The Physical Science Basis*, 1513–1766 (2023).
19. Y. Yang, S. Zhang, T. R. McVicar, H. E. Beck, Y. Zhang, B. Liu, Disconnection Between Trends of Atmospheric Drying and Continental Runoff. *Water Resour Res* **54** (2018).
20. J. T. Overpeck, B. Udall, Climate change and the aridification of North America. [Preprint] (2020). https://doi.org/10.1073/pnas.2006323117.
21. P. C. D. Milly, K. A. Dunne, Colorado River flow dwindles as warming-driven loss of reflective snow energizes evaporation. *Science (1979)* **367** (2020).
22. M. Berdugo, M. Delgado-Baquerizo, S. Soliveres, R. Hernández-Clemente, Y. Zhao, J. J. Gaitán, N. Gross, H. Saiz, V. Maire, A. Lehman, M. C. Rillig, R. V. Solé, F. T. Maestre, Global ecosystem thresholds driven by aridity. *Science (1979)* **367** (2020).
23. M. Delgado-Baquerizo, F. T. Maestre, A. Gallardo, M. A. Bowker, M. D. Wallenstein, J. L. Quero, V. Ochoa, B. Gozalo, M. García-Gómez, S. Soliveres, P. García-Palacios, M. Berdugo, E. Valencia, C. Escolar, T. Arredondo, C. Barraza-Zepeda, D. Bran, J. A. Carreira, M. Chaieb, A. A. Conceicao, M. Derak, D. J. Eldridge, A. Escudero, C. I. Espinosa, J. Gaitán, M. G. Gatica, S. Gómez-González, E. Guzman, J. R. Gutiérrez, A. Florentino, E. Hepper, R. M. Hernández, E. Huber-Sannwald, M. Jankju, J. Liu, R. L. Mau, M. Miriti, J. Monerris, K. Naseri, Z. Noumi, V. Polo, A. Prina, E. Pucheta, E. Ramírez, D. A. Ramírez-Collantes, R. Romao, M. Tighe, D. Torres, C. Torres-Díaz, E. D. Ungar, J. Val, W. Wamiti, D. Wang, E. Zaady, Decoupling of soil nutrient cycles as a function of aridity in global drylands. *Nature* **502** (2013).
24. N. Middleton, D. S. G. Thomas, World atlas of desertification. *World atlas of desertification*, doi: 10.2307/3060449 (1992).
25. C. H. B. PRIESTLEY, R. J. TAYLOR, On the Assessment of Surface Heat Flux and Evaporation Using Large-Scale Parameters. *Mon Weather Rev* **100**, 81–92 (1972).
26. H. L. Penman, Natural Evaporation from Open Water, Bare Soil and Grass. *Proc R Soc Lond A Math Phys Sci* **193** (1948).
27. J. L. Monteith, Evaporation and environment. *Symp Soc Exp Biol* **19**, 205–234 (1965).
28. R. G. Allen, L. S. Pereira, D. Raes, M. Smith, *Crop Evapotranspiration – Guidelines for Computing Crop Water Requirements* (Food and Agriculture Organization of the United Nations, Rome, Italy, 1998; http://www.fao.org/docrep/X0490E/x0490e00.HTM)*FAO Irrigation and drainage paper 56*.
29. W. H. Maes, P. Gentine, N. E. C. Verhoest, D. G. Miralles, Potential evaporation at eddy-covariance sites across the globe. *Hydrol Earth Syst Sci* **23**, 925–948 (2019).
30. C. M. Albano, J. T. Abatzoglou, D. J. McEvoy, J. L. Huntington, C. G. Morton, M. D. Dettinger, T. J. Ott, A Multidataset Assessment of Climatic Drivers and Uncertainties of Recent Trends in Evaporative Demand across the Continental United States. *J Hydrometeorol* **23**, 505–519 (2022).
31. C. Matsoukas, N. Benas, N. Hatzianastassiou, K. G. Pavlakis, M. Kanakidou, I. Vardavas, Potential evaporation trends over land between 1983-2008: Driven by radiative fluxes or vapour-pressure deficit? [Preprint] (2011). https://doi.org/10.5194/acp-11-7601-2011.
32. A. Barkhordarian, S. S. Saatchi, A. Behrangi, P. C. Loikith, C. R. Mechoso, A Recent Systematic Increase in Vapor Pressure Deficit over Tropical South America. *Scientific Reports 2019 9:1* **9**, 1–12 (2019).
33. Z. Fang, W. Zhang, M. Brandt, A. M. Abdi, R. Fensholt, Globally Increasing Atmospheric Aridity Over the 21st Century. *Earths Future* **10**, e2022EF003019 (2022).
34. D. L. Ficklin, K. A. Novick, Historic and projected changes in vapor pressure deficit suggest a continental-scale drying of the United States atmosphere. *Journal of Geophysical Research: Atmospheres* **122**, 2061–2079 (2017).
35. L. Lin, A. Gettelman, S. Feng, Q. Fu, Simulated climatology and evolution of aridity in the 21st century. *Journal of Geophysical Research: Atmospheres* **120**, 5795–5815 (2015).
36. C. Shenbin, L. Yunfeng, A. Thomas, Climatic change on the Tibetan Plateau: Potential evapotranspiration trends from 1961-2000. *Clim Change* **76**, 291–319 (2006).

37. C. Liu, D. Zhang, X. Liu, C. Zhao, Spatial and temporal change in the potential evapotranspiration sensitivity to meteorological factors in China (1960-2007). *Journal of Geographical Sciences* **22**, 3–14 (2012).
38. D. Luo, Z. Hu, L. Dai, G. Hou, K. Di, M. Liang, R. Cao, X. Zeng, An overall consistent increase of global aridity in 1970–2018. *Journal of Geographical Sciences* **33**, 449–463 (2023).
39. H. Sahour, M. Vazifedan, F. Alshehri, Aridity trends in the Middle East and adjacent areas. *Theor Appl Climatol* **142**, 1039–1054 (2020).
40. K. Ahmed, S. Shahid, X. Wang, N. Nawaz, N. Khan, Spatiotemporal changes in aridity of Pakistan during 1901-2016. *Hydrol Earth Syst Sci* **23**, 3081–3096 (2019).
41. M. Alfaro-Córdoba, H. G. Hidalgo, E. J. Alfaro, Aridity Trends in Central America: A Spatial Correlation Analysis. *Atmosphere 2020, Vol. 11, Page 427* **11**, 427 (2020).
42. A. Mamalakis, J. T. Randerson, J. Y. Yu, M. S. Pritchard, G. Magnusdottir, P. Smyth, P. A. Levine, S. Yu, E. Foufoula-Georgiou, Zonally contrasting shifts of the tropical rain belt in response to climate change. *Nature Climate Change 2021 11:2* **11**, 143–151 (2021).
43. A. Bárdossy, H. J. Caspary, Detection of climate change in Europe by analyzing European atmospheric circulation patterns from 1881 to 1989. *Theor Appl Climatol* **42**, 155–167 (1990).
44. T. G. Shepherd, Atmospheric circulation as a source of uncertainty in climate change projections. *Nature Geoscience 2014 7:10* **7**, 703–708 (2014).
45. IPCC, "Sixth Assessment Report (AR6)" (2022).
46. P. J. Borah, V. Venugopal, J. Sukhatme, P. Muddebihal, B. N. Goswami, Indian monsoon derailed by a North Atlantic wavetrain. *Science (1979)* **370** (2020).
47. J. A. Screen, I. Simmonds, Amplified mid-latitude planetary waves favour particular regional weather extremes. *Nat Clim Chang* **4** (2014).
48. K. E. Trenberth, A. Dai, G. Van Der Schrier, P. D. Jones, J. Barichivich, K. R. Briffa, J. Sheffield, Global warming and changes in drought. [Preprint] (2014). https://doi.org/10.1038/nclimate2067.
49. D. G. Miralles, P. Gentine, S. I. Seneviratne, A. J. Teuling, Land–atmospheric feedbacks during droughts and heatwaves: state of the science and current challenges. *Ann N Y Acad Sci* **1436** (2019).
50. S. Zhou, A. Park Williams, A. M. Berg, B. I. Cook, Y. Zhang, S. Hagemann, R. Lorenz, S. I. Seneviratne, P. Gentine, Land–atmosphere feedbacks exacerbate concurrent soil drought and atmospheric aridity. *Proc Natl Acad Sci U S A* **116** (2019).
51. A. Berg, K. Findell, B. Lintner, A. Giannini, S. I. Seneviratne, B. Van Den Hurk, R. Lorenz, A. Pitman, S. Hagemann, A. Meier, F. Cheruy, A. Ducharne, S. Malyshev, P. C. D. Milly, Land–atmosphere feedbacks amplify aridity increase over land under global warming. *Nature Climate Change 2016 6:9* **6**, 869–874 (2016).
52. N. Zeng, Drought in the Sahel. *Science (1979)* **302**, 999–1000 (2003).
53. D. L. Schumacher, J. Keune, P. Dirmeyer, D. G. Miralles, Drought self-propagation in drylands due to land–atmosphere feedbacks. *Nat Geosci* **15** (2022).
54. D. L. Schumacher, J. Keune, C. C. van Heerwaarden, J. Vilà-Guerau de Arellano, A. J. Teuling, D. G. Miralles, Amplification of mega-heatwaves through heat torrents fuelled by upwind drought. *Nat Geosci* **12** (2019).
55. M. Röthlisberger, L. Papritz, Quantifying the physical processes leading to atmospheric hot extremes at a global scale. *Nat Geosci*, doi: 10.1038/s41561-023-01126-1 (2023).
56. A. Koppa, J. Keune, D. Schumacher, K. Michaelides, M. Singer, S. Seneviratne, D. Miralles, Supplementary Materials: Global dryland self-expansion enabled by land–atmosphere feedbacks . (2023).
57. D. R. Cayan, T. Das, D. W. Pierce, T. P. Barnett, M. Tyree, A. Gershunova, Future dryness in the Southwest US and the hydrology of the early 21st century drought. *Proc Natl Acad Sci U S A* **107**, 21271–21276 (2010).
58. Y. Jiang, L. Zhou, C. J. Tucker, A. Raghavendra, W. Hua, Y. Y. Liu, J. Joiner, Widespread increase of boreal summer dry season length over the Congo rainforest. *Nature Climate Change 2019 9:8* **9**, 617–622 (2019).
59. J. Jiang, T. Zhou, Agricultural drought over water-scarce Central Asia aggravated by internal climate variability. *Nature Geoscience 2023 16:2* **16**, 154–161 (2023).
60. F. Lopes Ribeiro, M. Guevara, A. Vázquez-Lule, A. Paula Cunha, M. Zeri, R. Vargas, The impact of drought on soil moisture trends across Brazilian biomes. *Hazards Earth Syst. Sci* **21**, 879–892 (2021).
61. H. A. Barbosa, T. V. Lakshmi Kumar, L. R. M. Silva, Recent trends in vegetation dynamics in the South America and their relationship to rainfall. *Natural Hazards* **77** (2015).

62. S. E. Nicholson, C. Funk, A. H. Fink, Rainfall over the African continent from the 19th through the 21st century. *Glob Planet Change* **165** (2018).
63. T. J. Peterson, M. Saft, M. C. Peel, A. John, Watersheds may not recover from drought. *Science (1979)* **372** (2021).
64. J. Keune, D. L. Schumacher, D. G. Miralles, A unified framework to estimate the origins of atmospheric moisture and heat using Lagrangian models. *Geosci Model Dev* **15**, 1875–1898 (2022).
65. A. Koppa, J. Keune, D. A. MacLeod, M. Singer, R. Nieto, L. Gimeno, K. Michaelides, R. Rosolem, G. Otieno, A. Tadege, D. G. Miralles, A Lagrangian Analysis of the Sources of Rainfall Over the Horn of Africa Drylands. *Journal of Geophysical Research: Atmospheres* **128**, e2022JD038408 (2023).
66. J. E. Tierney, C. C. Ummenhofer, P. B. DeMenocal, Past and future rainfall in the Horn of Africa. *Sci Adv* **1** (2015).
67. A. P. Williams, E. R. Cook, J. E. Smerdon, B. I. Cook, J. T. Abatzoglou, K. Bolles, S. H. Baek, A. M. Badger, B. Livneh, Large contribution from anthropogenic warming to an emerging North American megadrought. *Science (1979)* **368** (2020).
68. B. F. Zaitchik, M. Rodell, M. Biasutti, S. I. Seneviratne, Wetting and drying trends under climate change. *Nature Water* **1** (2023).
69. P. Lal, A. Shekhar, M. Gharun, N. N. Das, Spatiotemporal evolution of global long-term patterns of soil moisture. *Science of the Total Environment* **867** (2023).
70. A. Gonsamo, P. Ciais, D. G. Miralles, S. Sitch, W. Dorigo, D. Lombardozzi, P. Friedlingstein, J. E. M. S. Nabel, D. S. Goll, M. O'Sullivan, A. Arneth, P. Anthoni, A. K. Jain, A. Wiltshire, P. Peylin, A. Cescatti, Greening drylands despite warming consistent with carbon dioxide fertilization effect. *Glob Chang Biol* **27** (2021).
71. Z. Chen, W. Wang, A. Cescatti, G. Forzieri, Climate-driven vegetation greening further reduces water availability in drylands. *Glob Chang Biol* **29** (2023).
72. L. Samaniego, S. Thober, R. Kumar, N. Wanders, O. Rakovec, M. Pan, M. Zink, J. Sheffield, E. F. Wood, A. Marx, Anthropogenic warming exacerbates European soil moisture droughts. *Nat Clim Chang* **8** (2018).
73. A. Koppa, Data: Global dryland self-expansion enabled by land-atmosphere feedbacks. doi: 10.5281/ZENODO.10408319 (2023).
74. J. Keune, A. Koppa, D. Miralles, FLEXPART–ERA-Interim simulations with 3 million parcels globally (1979–2019). doi: 10.5281/ZENODO.6947524.

Acknowledgments: The computational resources and services used in this work were provided by the VSC (Flemish Supercomputer Center), funded by the Research Foundation, Flanders (FWO), and the Flemish Government.

Funding: The study was funded by the European Union Horizon 2020 Programme (DOWN2EARTH, 869550). J.K. is grateful for the support from the Research Foundation Flanders (FWO) under grant no. 1244122N.

Author contributions: A.K. and J.K. conceived the idea. A.K., J.K., and D.G.M. designed the experiments. J.K. conducted the global Lagrangian model simulations with help from A.K. A.K. performed the primary analysis of dryland self-expansion with extensive inputs from J.K., D.G.M., and D.L.S. A.K. drafted the first version of the manuscript with significant contributions from J.K. and D.G.M. All co-authors contributed to the interpretation of results and writing of the final version.

Competing interests: The authors declare no competing interests.

Data and materials availability: All outputs and code to reproduce the final figures are available at (*73*). The dataset of FLEXPART–ERA-Interim simulations containing 3 million parcels used for tracking heat and moisture in this study are available at (*74*).